Formation of traveling waves in nematics due to material parameter ramps

Karen K. Vardanyan*
Department of Physics & Geology, The University of Texas-Pan American, Edinburg, Texas 78539, USA

Daniel R. Spiegel
Department of Physics & Astronomy, Trinity University, San Antonio, Texas 78212, USA
(Received 21 February 2007; published 6 September 2007)

We propose a simple one-dimensional linear model to describe the formation of localized traveling waves due to material parameter ramps in nematic liquid crystals. We assume that due to some external perturbation the material parameters (conductivity, dielectric constants, viscosity, elasticity) of the liquid crystal become slowly varying functions of position. Temperature gradient in localized regions induced by a laser beam could be one such perturbation. We obtain a 4×4 system of electrohydrodynamic equations [partial derivative equations (PDE) with respect to time and position]. At first we assume that all parameters change from their nonperturbed value by the same ramp function. Then, to reveal the parameters which slowly change are predominant in the formation of localized traveling waves, we obtain four more systems of equations. Each time we assume that just one of the material parameters changes while the others are held constant. Accordingly, by reducing 4×4 systems of equations into one equation and using a WKB-like approach for nonuniform media, we obtain the relevant dispersion relations. We show that ramps of elasticity and dielectric parameters play the dominant role in the formation of localized traveling waves in nonuniform nematic media.

DOI: 10.1103/PhysRevE.76.031703 PACS number(s): 83.80.Xz, 47.54.−r, 47.65.−d, 47.35.−i

I. INTRODUCTION

During recent years there has been considerable interest in electroconvection (EC) within nematic liquid crystal (NLC). EC investigations have been carried out for both alignment types in nematic liquid crystal cells: planar [1–4], and homeotropic [5–8]. The most familiar results of EC are formation of normal stationary Williams rolls (William domain mode: WDM) [9], and dynamic rolls (dynamic scattering mode: DSM) [10] with the characteristic wavelengths about equal to the cell thickness. These rolls have been observed in 4-methoxy-benzilidene-4-butylaniline (MBBA) NLC, which has negative dielectric anisotropy and positive conductivity anisotropy, in cells with a planar configuration. One-dimensional modeling of these rolls was carried out by Carr [11] and Helfrich [12]. Boundary conditions were introduced later by Penz and Ford [13] and Pikin [14]. As a result two-dimensional modeling of the rolls were carried out. Goossens discussed one- and two-dimensional models and the boundary condition problem for the two-dimensional case [15]. However, recently there have been several reports of formation of spatially localized states, known as pulses, in nematics. Dennin and co-workers obtained spontaneously arising worm pulses near threshold in I52 NLC [16–19]. Joets and Ribotta reported observations of small traveling waves regions near the EC threshold in MBBA [20]. Rolls traveling in the same direction were observed within inclusions. The direction of travel for different inclusions varied randomly to the right or left along the director. Brand and co-workers observed spatially localized rolls working at a temperature close to a smectic-nematic phase transition in the liquid crystal 10E6 with negative conductivity anisotropy [21]. Giebink, *et al.* recently reported that a continuous laser beam (488 nm) with a v-shaped ramp intensity profile and with a cross section comparable to the WDM wavelength size generates counterpropagating waves along the director traveling in dye-doped MBBA cells with a planar configuration [22]. The result was obtained working 10–20% below WDM threshold voltage (low frequency voltages; 70–100 Hz dc approximation) for a laser-free sample. The rolls moving at frequencies of tenths of Hz were confined within a robust pulse shaped as an ellipse with the semimajor axis parallel to the nematic director, and with a typical size of several WDM wavelengths. In work [23], Spiegel, Johnson, and Saucedo reported an experiment in which a controlled spatial ramp of the temperature, caused by a ramp-shaped intensity laser (488 nm) profile, produces spatially localized electroconvection rolls in dye-doped MBBA cells with a planar configuration. The authors of Refs. [22,23] proposed that the theoretical modeling of these pulses should be based on control-parameters ramp models. Periodic spatial patterns have been observed and discussed in other systems as well: fluids [24–26], crystal growth [27], and chemical-reaction-diffusion systems with autocatalytic elements [28,29]. However, the theoretical work directed towards an understanding of the wavelength selection process [26,30–35] has dealt for the most part with Rayleigh-Benard convection (RBC) and the Taylor systems in simple fluids [24–26]. Cross and co-workers [31,35] have clarified that nonperiodic boundary conditions can influence the band of allowed wavelengths but in general do not select a unique wavelength. Pomeau and Manneville [34] introduced the concept of a small curvature into quasi-infinite axis-symmetric systems to single out specific wavelength state. Kramer *et al.* [36] using WKB-like approach analyzed wavelength selection for a simple reaction-diffusion equations system with periodicity in one dimension and slowly varying external parameters. Such

*Author to whom correspondence should be addressed.

ramps lead to a unique final state acting as selecting boundaries. Motivated by the experimental results reported in [22] (see above) we propose a one-dimensional material parameter ramp model describing the formation of patterns under applied external constant force in a nonuniform media. Liquid crystal cell with planar configuration and under applied external constant electric field represents such a media. Note that we do not try to compare our results with the experimental data obtained in [22], rather motivated by these results we intend to examine the role of different material parameters variation in pattern formation in NLC with negative dielectric and positive conductivity anisotropies. In this work we apply Kramer's WKB-like approach to the electrohydrodynamic equations for NLC [15] considering the fact that the material parameters slowly vary in a localized region. Historically, WKB method first was applied to the time-independent one-dimensional Schrodinger equation [37]:

$$(d^2\psi/dx^2) + q^2(x)\psi = 0,$$

$$q = \sqrt{K^2 - U(x)},$$

$$K^2 = (2M/\hbar)E_k, \quad \hbar = h/2\pi,$$

$$U = (2M/\hbar)V_p. \tag{1}$$

This equation describes the quantum mechanical motion of a particle with M mass and E_k energy in one dimension under the influence of a V_p potential. Here ψ is the wave function and h is Planck's constant. One can look for an approximate solution of Eq. (1) in the form

$$\psi = \exp[\varphi(x)]. \tag{2}$$

Here φ is the phase of the exponential function. Substitution of Eq. (2) into Eq. (1) leads to the result

$$\psi \approx q^{-1/2} \exp\left(\pm i \int q dx\right). \tag{3}$$

The validity of this result is given by

$$\left|\frac{(\partial U/\partial x)}{2q^3}\right| \ll 1. \tag{4}$$

It is clear that the method is applicable only when the variation of $U(x)$ over a wavelength becomes smaller. Note that the method fails when either the variation of the potential function becomes bigger or when q vanishes. Note that we apply WKB-like method to separate material parameters. Considering the fact that "real-world" patterns in nature will essentially never occur in perfectly uniform media, our method should be applicable to other pattern-forming systems like RBC and Taylor-vortex flow [24–26]. It is important to indicate that in [22,23] the authors reported that the localized pulse has a typical size of several wavelengths. However from a theoretical perspective it is preferable when the overall size of the localized region is much larger than the rolls wavelength. Most importantly, for this case one can apply WKB-like approach to the differential equations characterizing the system (as discussed above). In our calculations we assume that a localized ellipse-shaped pulse length is larger than characteristic WDM wavelength by two orders of magnitude. Note that due to the small time scales considered in our model we ignore the heat transfer effects and consider isothermal process.

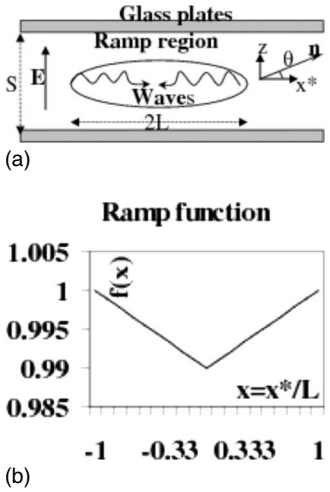

FIG. 1. (a) Schematics of the liquid crystal cell; S—cell thickness; E—applied electric field vector; n—nematic's director; θ—molecules distortion angle; $2L$—localized ramp region's length; x^*, z—Cartesian coordinate system; the sinusoidal-shape lines inside the localized region represent the counterpropagating waves. (b) Dependence of ramp function $f(x)$ vs normalized coordinate x.

In Fig. 1(a) a schematics of NLC cell with planar configuration is depicted. We assume that the length of localized pulse (in x direction) $2L$ is 100 times larger than the WDM wavelength which is equal to twice the cell thickness S. For instance, if the cell has a 40 micron thickness then the pulse has 0.8 cm length. Note that the glass plate length (in x direction) is assumed to be a few orders of magnitude larger than pulse length, so we have a quasi-infinite system with uncertain boundary conditions.

II. VARIATION OF MULTIPLE PARAMETERS

At first we introduce four original electrohydrodynamic equations of nematics [15]. The first equation is from electrostatics (Gauss law),

$$\mathrm{div}\,\vec{D} = 4\pi q,$$

$$\vec{D} = \hat{\varepsilon}\vec{E}, \quad \hat{\varepsilon} \equiv \varepsilon_{uv} = \varepsilon_r \delta_{uv} + \varepsilon_a n_u n_v, \quad \varepsilon_a = \varepsilon_p - \varepsilon_r,$$

$$\delta_{uv} = \begin{cases} 1 & \text{when } u = v, \\ 0 & \text{when } u \neq v, \end{cases} \quad u, v = 1,2,3. \tag{5}$$

Here E is the electric field, n the director, q the charge density, D the electric field in dielectric, ε_{uv} the dielectric parameter tensor, δ_{uv} the unity matrix, and ε_p and ε_r are dielectric constants parallel and perpendicular to the director directions, respectively. The second equation is from electrodynamics (continuity equation),

$$\partial q/\partial t + \mathrm{div}\,\vec{J} = 0,$$

$$\vec{J} = \hat{\sigma}\vec{E}, \quad \hat{\sigma} \equiv \sigma_{uv} = \sigma_r \delta_{uv} + \sigma_a n_u n_v, \quad \sigma_a = \sigma_p - \sigma_r. \quad (6)$$

Here J is the current density, $\sigma_{u\nu}$ the conductivity tensor, and σ_p and σ_r are conductivity constants parallel and perpendicular to the director directions, respectively. Note that for the uniform medium geometry and small distortion angle the electric field and director vectors have the following components [see Fig. 1(a)]:

$$\vec{E} = \{E_x(x,t), 0, E\},$$

$$\vec{n} = \{1, 0, \theta(x,t)\}. \quad (7)$$

The third equation is the rotational equivalent of the second law of motion for the director,

$$\vec{\Gamma}_e + \vec{\Gamma}_\nu = I(d/dt)\vec{\Omega},$$

$$I(d/dt)\vec{\Omega} \approx \vec{0}, \quad \vec{\Gamma}_e = -\vec{n} \times (\delta F/\delta \vec{n}),$$

$$\vec{\Gamma}_\nu = -\vec{n} \times (\gamma_1 \vec{N} + \gamma_2 \hat{A} \cdot \vec{n}),$$

$$\Omega = \vec{n} \times (d\vec{n}/dt), \quad F = F_e + F_d,$$

$$F_e = 0.5[K_{11}(\text{div } \vec{n})^2 + K_{22}(\vec{n} \cdot \text{rot } \vec{n})^2 + K_{33}(\vec{n} \times \text{rot } \vec{n})^2],$$

$$F_d = -\frac{\varepsilon_a}{8\pi}(\vec{n} \cdot \vec{E})^2, \quad \vec{N} = d\vec{n}/dt - 0.5(\text{rot } \vec{V} \times \vec{n}),$$

$$\hat{A} \equiv A_{u\nu} = A_{\nu u} = 0.5(\partial V_u/\partial r_\nu + \partial V_\nu/\partial r_u), \quad u, \nu = 1,2,3,$$

$$\vec{V} = \{0, 0, V_z(x)\}, \quad r_u, r_\nu = x, y, z. \quad (8)$$

Where Γ_e and Γ_ν are elastic and viscous torques per unit volume on the director, respectively, I is the moment of inertia per unit volume, Ω is the angular velocity of the director, F is free energy density, F_e the elastic component of free energy density, F_v the viscous component of free energy density, $\boldsymbol{V}$ the local velocity of the fluid. Note that we neglect the internal term in the equation as it is negligible in comparison with elastic and viscous terms (about fourteen orders smaller) [15]. The fourth equation is the z component of the equation of motion for the moving fluid

$$\mu(d\vec{V}/dt) = q\vec{E} + \text{div } \hat{t},$$

$$\mu(d\vec{V}/dt) \approx \vec{0}, \quad (\text{div } \hat{t})_u = (\partial/\partial r_\nu) t_{\nu u} \equiv t_{\nu u,\nu},$$

$$t_{u\nu} = -p\delta_{u\nu} - (\partial F/\partial n_{w,u}) n_{w,\nu} + \bar{t}_{u\nu},$$

$$(\partial F/\partial n_{w,u}) n_{w,\nu} \approx 0,$$

$$\bar{t}_{u\nu} = \alpha_1 n_k n_p A_{kp} n_u n_\nu + \alpha_2 n_u N_\nu + \alpha_3 n_\nu N_u + \alpha_4 A_{u\nu} + \alpha_5 n_u n_k A_{k\nu} + \alpha_6 n_\nu n_k A_{ku},$$

$$u, \nu, w, k, p = 1,2,3. \quad (9)$$

The left-hand side is the inertial term (μ-fluid density) which is negligible in comparison with right-hand side terms [15]. The first term is the external electric force acting on the fluid. The second term on the right-hand side is the force the due to stress associated with the fluid. And $t_{vu,v}$ is the v component of this force. Here $t_{u\nu}$ is the stress tensor. The first term in the expression of this tensor is the hydrostatic pressure (p). The second term is the stress connected with the free energy. For small deformations (such as our case) this term plays no role and can be neglected [15]. The third term is the viscous part of the stress. In the expression for this part α_u is viscosity coefficients associated with the stress. Note that a small angle distortion assumption [see Eq. (7)] yields the following z component of Eq. (9):

$$(\partial/\partial x)\bar{t}_{xz} + qE = 0,$$

$$\bar{t}_{xz} = \alpha_2(\partial\theta/\partial t) + 0.5[-\alpha_2 + \alpha_4 + \alpha_5](\partial/\partial x)V_z,$$

$$\eta_1 = 0.5[-\alpha_2 + \alpha_4 + \alpha_5]. \quad (10)$$

For nonuniform medium the material parameters are not constants. We assume they are slowly varying functions of the spatial coordinate. The word slowly needs further clarification, which we will do after introducing some new functions. First of all we would like to obtain a dimensionless spatial coordinate and time. We normalize coordinate x^* and time t^* as $x = x^*/L$ [see Fig. 1(a)], and $t = t^*/P$. P could be a very short period of time: 10^{-3} seconds, which is less than the reciprocal of the applied low frequency (70–100 Hz) electric field by one order of magnitude. Then we introduce a small parameter $\varepsilon \ll 1$ which is of the same order of the fraction $\lambda_{WDM}/2L = 10^{-2}$. The modified coordinate and time can be obtained now as $X = \varepsilon x$ and $T = \varepsilon^2 t$. Note that the time scale is "slower" since the material parameters are independent of time. In this model we assume that all material parameters vary with a same linear ramp function [see Fig. 1(b)]:

$$f(x) \equiv \tilde{f}(X) = \begin{cases} 1, & x > 1 \\ \varepsilon x + 1 - \varepsilon, & 0 \leqslant x \leqslant 1 \\ -\varepsilon x + 1 - \varepsilon, & -1 \leqslant x \leqslant 0 \\ 1, & x < -1 \end{cases},$$

$$(d/dx)f(x) = \begin{cases} 0, & x > 1 \\ \varepsilon, & 0 \leqslant x \leqslant 1 \\ -\varepsilon, & -1 \leqslant x \leqslant 0 \\ 0, & x < -1 \end{cases},$$

$$(d^n/dx^n)f(x) = 0, \quad n = 2,3,4 \ldots . \quad (11)$$

One can see from Fig. 1(a) that the localized region has a symmetry to the z axis. Thus in our calculations we consider x varying from 0 to 1. Now we can clarify the expression "slowly varying." One can see from Eq. (11) that the first derivative of this function, which indicates the function's change rate, is a small number in the order of 10^{-2}. At first we assume that all material parameters slowly vary with the

same ramp function $f(x)$ and treat the electrohydrodynamic equations [Eqs. (5), (6), (8), and (10)] for this case. Then we will assume that only one parameter varies while the others are held constant. We apply this approach to examine the potential of formation of traveling waves as a result of either combined multiparameter perturbation or a single parameter perturbation. By applying this approach we intend also to reveal the parameters which perturbation could lead into formation of traveling waves observed and reported in work [22]. Note that in reality the temperature dependence (which causes the spatial variations) is different for the parallel (increases) and perpendicular (decreases) components of the dielectric parameter. But considering the facts that for the most nematics the change in magnitude for any of the relevant parameters is less than one percent for an increment of five degrees in Celsius, and that the authors in [22] applied only a change of one degree, we treat all changes (such as both components of dielectric parameter) as a perturbation in temperature. So we assume that all parameters vary in a similar way. For multiparameter spatial variations we have $\alpha_2(x)=\alpha_2 f(x)$, $\alpha_4(x)=\alpha_4 f(x)$, $\alpha_5(x)=\alpha_5 f(x)$, $\gamma_1(x)=\gamma_1 f(x)$, $\varepsilon_p(x)=\varepsilon_p f(x)$, $\varepsilon_r(x)=\varepsilon_r f(x)$, $\varepsilon_a(x)=\varepsilon_a f(x)$, $\sigma_p(x)=\sigma_p f(x)$, $\sigma_r(x)=\sigma_r f(x)$, $\sigma_a(x)=\sigma_a f(x)$, $K_{33}(x)=K_{33} f(x)$, where the constants are the material parameters values for uniform medium. By employing these functions into Eqs. (5), (6), (8), and (10) we obtain 4×4 partial derivative equations (PDE) system which reduces to a PDE,

$$-a_m(x)\theta_{xxxt}-b_m\theta_{xxt}+c_m(x)\theta_{xt}+d_m\theta_t+g_m\theta_{tt}+h_m(x)\theta_{xtt}+m_m(x)\theta_x+p_m\theta-r_m(x)\theta_{xxx}-s_m\theta_{xx}=0,$$

$$a_m(x)=K_{33}f(x),$$

$$b_m=2K_{33}\varepsilon,$$

$$c_m(x)=[\varepsilon_H E^2+\sigma_{HV}\eta^*]f(x),$$

$$\sigma_{HV}=\sigma_p 4\pi/\varepsilon_p,\quad \varepsilon_H=-\varepsilon_a\varepsilon_r/4\pi\varepsilon_p,$$

$$d_m=[\varepsilon_H E^2+\sigma_{HV}\eta^*]\varepsilon,$$

$$\eta^*=\gamma_1-\alpha_2{}^2/\eta_1,$$

$$g_m=\eta^*\varepsilon,$$

$$h_m=\eta^* f(x),$$

$$m_m(x)=[\varepsilon_{HV}\sigma_H+\sigma_{HV}\varepsilon_H]E^2 f(x),$$

$$\varepsilon_{HV}=\varepsilon_a/\varepsilon_p+\alpha_2/\eta_1,$$

$$\sigma_H=\sigma_p[\varepsilon_r/\varepsilon_p-\sigma_r/\sigma_p],$$

$$p_m=[\varepsilon_{HV}\sigma_H+\sigma_{HV}\varepsilon_H]E^2\varepsilon,$$

$$r_m(x)=\sigma_{HV}K_{33}f(x),$$

$$s_m=2\sigma_{HV}K_{33}\varepsilon. \tag{12}$$

Here the subscripts in the first line indicate partial derivatives of the distortion angle θ with respect to the coordinate x and time t. For MBBA at room temperature the material parameters for uniform medium are as follows [13,15]: $\alpha_2=-0.8$ P, $\alpha_4=0.8$ P, $\alpha_5=0.5$ P, $\gamma_1=0.8$ P, $\varepsilon_p=4.7$, $\varepsilon_r=5.4$, $\sigma_p=13.5\ \mathrm{sec}^{-1}$, $\sigma_r=9\ \mathrm{sec}^{-1}$, $K_{33}=10^{-6}$ dyne, and we assume that the control parameter E is changing within the range of zero and 10 Statvolt/cm. We apply an WKB-like approach [36,37] and seek a solution of the form

$$\theta=\theta_0\exp(i\varphi)+\theta_1\exp(i\varphi)+\ldots,$$

$$\theta_0(x,t)=\varepsilon^0\tilde{\theta}_0(X,T),\quad \theta_{0x}=\varepsilon\tilde{\theta}_{0X},$$

$$\theta_1(x,t)=\varepsilon\tilde{\theta}_1(X,T),$$

$$\varphi(x,t)=\varepsilon^{-1}\tilde{\varphi}(X,T),$$

$$\varphi_x\equiv k=\tilde{\varphi}_X,\quad \varphi_{xx}\equiv k_x=\varepsilon\tilde{\varphi}_{XX},$$

$$\varphi_t\equiv-\omega=\varepsilon\tilde{\varphi}_T. \tag{13}$$

Where φ is a complex phase, k and ω are complex wave number and frequency, respectively. Note that we neglect all terms with ε^2 and higher orders. We substitute Eq. (13) into Eq. (12) and equate to zero terms of successive orders of the small parameter. The hierarchy for ε^0 and ε^1 becomes, respectively,

$$[ir_m(x)k^3+s_m k^2+im_m(x)k+p_m]\theta_0=0, \tag{14a}$$

$$[ir_m(x)k^3+s_m k^2+im_m(x)k+p_m]\theta_1+[a_m(x)k^3\omega-ib_m k^2\omega+c_m(x)k\omega-id_m\omega+3r_m(x)kk_x-is_m k_x]\theta_0+[3r_m(x)k^2+i2s_m k+m_m(x)]\theta_{0x}=0. \tag{14b}$$

III. CONSTANT MATERIAL PARAMETERS MODEL

For constant parameters $f(x)=1$ and Eq. (12) converts to a PDE which describes classical William's rolls [15] mode for a system without nonuniform localized region,

$$a\theta_{xtt}-b\theta_{xxxt}+c\theta_{xt}-d\theta_{xxx}+g\theta_x=0,$$

$$a=\eta^*,$$

$$b=K_{33},$$

$$c=\eta^*\sigma_{HV}+\varepsilon_H E^2,$$

$$d=\sigma_{HV}K_{33},$$

$$g=[\varepsilon_{HV}\sigma_H-\sigma_p\varepsilon_a\varepsilon_r/\varepsilon_p{}^2]E^2, \tag{15}$$

Hence, by introducing

$$\theta=\theta_0\exp[\varphi(x,t)],$$

$$\varphi = i[kx - \omega t], \tag{16}$$

we obtain the dispersion relationship for Eq. (15),

$$-iak\omega^2 + [bk^3 + ck]\omega + [idk^3 + igk] = 0. \tag{17}$$

For MBBA with its material parameters at room temperature (see above)

$$[bk^2 + c]^2 > 4a[dk^2 + g]. \tag{18}$$

Therefore the two roots of Eq. (17) are purely imaginary, which indicate that there is no temporal oscillation of the distortion angle in the uniform medium. The negative root indicates that the distortion angle amplitude decreases exponentially in time and approaches a constant value asymptotically. The positive root indicates that the amplitude increase in time exponentially so that the condition of small angle distortion is not valid anymore. By equating positive root to zero one can obtain the equation relating wave number to threshold field,

$$k^2 = -g/d,$$

$$E = E_{th}. \tag{19}$$

IV. VARIABLE CONDUCTIVITY MODEL

Now we consider that only the conductivity of the medium varies, $\sigma_p(x) = \sigma_p f(x)$, $\sigma_r(x) = \sigma_r f(x)$, $\sigma_a(x) = \sigma_a f(x)$, while the other parameters are held constant. We obtain the following PDE for this case from the electrohydrodynamic equations (see above),

$$-a_c\theta_{xxxxt} + b_c(x)\theta_{xxt} + c_c\theta_{xxtt} - d_c(x)\theta_{xxxx} + g_c(x)\theta_{xx} - h_c\theta_{xxx} + m_c\theta_x + p_c\theta_{xt} = 0,$$

$$a_c = K_{33},$$

$$b_c(x) = \varepsilon_H E^2 + \sigma_{HV}\eta^* f(x),$$

$$c_c = \eta^*,$$

$$d_c(x) = \sigma_{HV}K_{33}f(x),$$

$$g_c(x) = [\varepsilon_{HV}\sigma_H + \sigma_{HV}\varepsilon_H]E^2 f(x),$$

$$h_c = 2\sigma_{HV}K_{33}\varepsilon,$$

$$m_c = 2[\varepsilon_{HV}\sigma_H + \sigma_{HV}\varepsilon_H]E^2\varepsilon,$$

$$p_c = 2\sigma_{HV}\varepsilon. \tag{20}$$

By substituting Eq. (13) into Eq. (20) we obtain the hierarchy for the small parameter successive orders:

$$[-d_c(x)k^4 + ih_ck^3 - g_c(x)k^2 + im_ck]\theta_0 = 0, \tag{21a}$$

$$[-d_c(x)k^4 + ih_ck^3 - g_c(x)k^2 + im_ck]\theta_1 + [ia_ck^4\omega + ib_c(x)k^2\omega + i6d_c(x)k^2k_x + ig_c(x)k_x + 3h_ckk_x + p_ck\omega]\theta_0 + [i4d_c(x)k^3 + 3h_ck^2 + i2g_c(x)k + m_c]\theta_{0x} = 0. \tag{21b}$$

V. VARIABLE VISCOSITY MODEL

By assuming that the viscosities of the medium varies slowly, $\alpha_2(x) = \alpha_2 f(x)$, $\alpha_4(x) = \alpha_4 f(x)$, $\alpha_5(x) = \alpha_5 f(x)$, $\gamma_1(x) = \gamma_1 f(x)$, while the other parameters are held constant, we obtain PDE

$$-a_\nu\theta_{xxxt} + b_\nu(x)\theta_{xt} + c_\nu(x)\theta_{xtt} + d_\nu\theta_{tt} - g_\nu\theta_{xxx} + h_\nu\theta_x + m_v\theta_t = 0,$$

$$a_\nu = K_{33},$$

$$b_\nu(x) = \varepsilon_H E^2 + \sigma_{HV}\eta^* f(x),$$

$$c_\nu(x) = \eta^* f(x),$$

$$d_\nu = \eta^*\varepsilon,$$

$$g_\nu = K_{33}\sigma_{HV},$$

$$h_\nu = [\varepsilon_{HV}\sigma_H + \sigma_{HV}\varepsilon_H]E^2,$$

$$m_\nu = \eta^*\sigma_{HV}\varepsilon. \tag{22}$$

By substituting Eq. (13) into Eq. (22) we obtain

$$[ig_\nu k^3 + ih_\nu k]\theta_0 = 0, \tag{23a}$$

$$[ig_\nu k^3 + ih_\nu k]\theta_1 + [a_\nu k^3\omega + b_\nu(x)k\omega + 3g_\nu kk_x - im_\nu\omega]\theta_0 + [3g_\nu k^2 + h_\nu]\theta_{0x} = 0. \tag{23b}$$

VI. VARIABLE DIELECTRIC MODEL

By assuming that dielectric parameters of the medium vary slowly, $\varepsilon_p(x) = \varepsilon_p f(x)$, $\varepsilon_r(x) = \varepsilon_r f(x)$, $\varepsilon_a(x) = \varepsilon_a f(x)$, while the other parameters are held constant, we obtain PDE

$$-a_d(x)\theta_{xxxxt} + b_d(x)\theta_{xxt} + c_d(x)\theta_{xt} + d_d(x)\theta_{xxtt} + g_d(x)\theta_{xx} + h_d\theta_x - m_d\theta_{xxxt} + p_d\theta_{xtt} - r_d\theta_{xxxx} = 0,$$

$$a_d(x) = K_{33}f(x),$$

$$b_d(x) = \varepsilon_H E^2 f^2(x) + \sigma_{HV}\eta^*,$$

$$c_d(x) = 4\varepsilon_H E^2 f(x)\varepsilon,$$

$$d_d(x) = \eta^* f(x),$$

$$g_d(x) = [\varepsilon_{HV}\sigma_H + \sigma_{HV}\varepsilon_H]E^2 f(x),$$

$$h_d = 2[\varepsilon_{HV}\sigma_H + \sigma_{HV}\varepsilon_H]E^2\varepsilon,$$

$$m_d = 2K_{33}\varepsilon,$$

$$p_d = 2\eta^*\varepsilon,$$

$$r_d = \sigma_{HV}K_{33}. \tag{24}$$

The substitution of Eq. (13) into Eq. (24) yields

$$[-r_d k^4 - g_d(x)k^2 + ih_d k]\theta_0 = 0, \tag{25a}$$

$$[-r_d k^4 - g_d(x)k^2 + ih_d k]\theta_1 + [ia_d(x)k^4\omega + ib_d(x)k^2\omega + c_d(x)k\omega + ig_d(x)k_x + m_d k^3\omega + i6r_d k^2 k_x]\theta_0 + [i4r_d k^3 + i2g_d(x)k + h_d]\theta_{0x} = 0. \tag{25b}$$

VII. VARIABLE ELASTICITY PARAMETER MODEL

At this time we assume that the bend elasticity of the medium varies slowly, $K_{33}(x)=K_{33}f(x)$, while the other parameters are held constant. This assumption yields PDE

$$-a_e(x)\theta_{xxxt} - b_e\theta_{xxt} + c_e\theta_{xtt} - d_e(x)\theta_{xxx} - g_e\theta_{xx} + h_e\theta_{xt} + m_e\theta_x = 0,$$

$$a_e(x) = K_{33}f(x),$$

$$b_e = 2K_{33}\varepsilon,$$

$$c_e = \eta^*,$$

$$d_e(x) = \sigma_{HV}K_{33}f(x),$$

$$g_e = 2\sigma_{HV}K_{33}\varepsilon,$$

$$h_e = \varepsilon_H E^2 + \sigma_{HV}\eta^*,$$

$$m_e = [\varepsilon_{HV}\sigma_H + \sigma_{HV}\varepsilon_H]E^2. \tag{26}$$

The substitution of Eq. (13) into Eq. (26) yields

$$[id_e(x)k^3 + g_e k^2 + im_e k]\theta_0 = 0, \tag{27a}$$

$$[id_e(x)k^3 + g_e k^2 + im_e k]\theta_1 + [a_e(x)k^3\omega - ib_e k^2\omega + 3d_e(x)kk_x - ig_e k_x + h_e k\omega]\theta_0 + [3d_e(x)k^2 - i2g_e k + m_e]\theta_{0x} = 0. \tag{27b}$$

VIII. RESULTS AND DISCUSSIONS

First of all let us note that when $f(x)=1$ (outside of the localized region, where the medium is uniform) Eqs. (12), (20), (22), (24), and (26) convert to constant parameters model, Eq. (15). Equations (14a), (21a), (23a), (25a), and (27a) are polynomial equations with respect to the complex wave number. We are interested in the positive roots of these equations. In Fig. 2 the dependence of real (oscillatory) wave number versus coordinate at different applied field values is depicted for all models. As one can see, for multiparameter, viscosity, and conductivity models the wave number is a constant regarding to the spatial coordinate. This is the case for the constant parameters model described above. Note that one can obtain the same dependence using Eq. (19), where each value of the applied field can be considered as a threshold value for a specific NLC cell thickness, since the latter is half of the wavelength [15]. For the dielectric model the wave number increases slowly and becomes a constant-parameter model value at the localized region limit. The wave number for elasticity model shows the same behavior by decreasing. We will see soon that these two models lead to the formation of traveling waves. In Fig. 3 the slopes of wave number coordinate dependence at different field values for dielectric and elasticity models are illustrated. One can see that for both cases the slope absolute value increases with the increase of the applied field, so the rate of change of wavelength versus coordinate decreases. Eqs. (14a), (21a), (23a), (25a), and (27a) eliminate terms with θ_1 in Eqs. (14b), (21b), (23b), (25b), and (27b), which become differential equations for the amplitude θ_0 with the solution

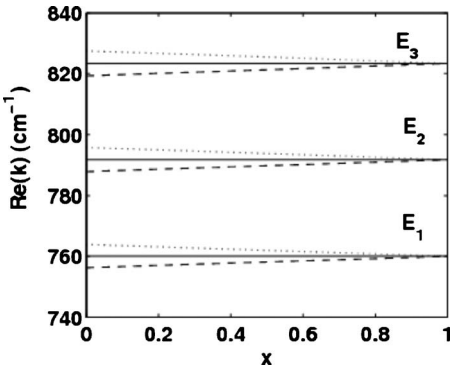

FIG. 2. Dependence of the real wave number versus normalized coordinate at three different values of applied electric field: E_1 =2.4 statvolt/cm, E_2=2.5 statvolt/cm, E_3=2.6 statvolt/cm; dotted line—elasticity model; solid line—multiparameter, viscosity, and conductivity models; dashed line—dielectric model.

$$\theta_0 = \text{const}\exp\left\{-\int [\alpha(x)/\beta(x)]dx\right\}. \tag{28}$$

Here $\alpha(x)$ and $\beta(x)$ are coefficients of θ_0 and θ_{0x}, respectively. If the dispersion relations and initial conditions are known one can obtain the exact solutions for the amplitude θ_0. Note that one can obtain the dispersion relations from Eqs. (14b), (21b), (23b), (25b), and (27b) by equating $\alpha(x)$ coefficients to zero only when either the coefficients of $\beta(x)$ are zero or θ_{0x} itself is zero. Since the $\beta(x)$ coefficients are

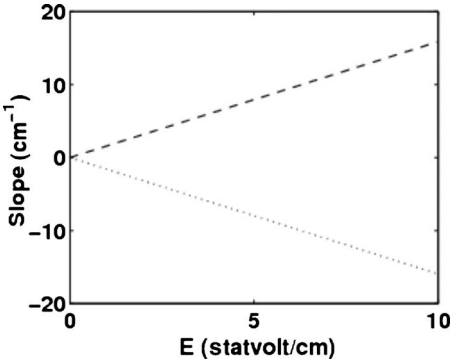

FIG. 3. Real wave number's slope as a function of applied electric field; dotted line—elasticity model; dashed line—dielectric model.

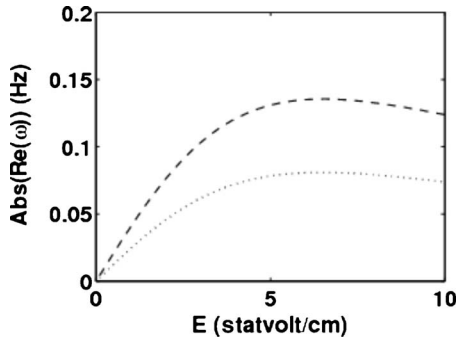

FIG. 4. Dependence of the absolute values of real frequency versus applied electric field; dotted line—elasticity model; dashed line—dielectric model (the values of the real frequency are negative for this case).

not zero one can obtain the dispersion relations only when θ_{0x} is zero. To achieve this we assume that the material parameters ramps affect just the phase of the distortion angle but not the amplitude. Now in Eq. (13) for θ_0 and θ_1, the coordinate and time change, in the same "very slow" way, so that they can be considered as constants,

$$\theta_0(x,t) = \varepsilon^0 \tilde{\theta}_0(\varepsilon^2 x, \varepsilon^2 t), \quad \theta_{0x} = \varepsilon^2 \tilde{\theta}_{0X} \approx 0,$$

$$\theta_1(x,t) = \varepsilon \tilde{\theta}_1(\varepsilon^2 x, \varepsilon^2 t). \tag{29}$$

After equating $\alpha(x)$ coefficients to zero one can see from Eqs. (14b), (21b), and (23b) that, due to the fact of k_x being zero for the multiparameter, conductivity, and viscosity models, the frequency for these cases is zero as well. This result is expected from the above discussion, and shows that (similar to the constant parameters model) there is no oscillation in time for the distortion angle. From Eqs. (25b) and (27b) we obtain the dispersion relations for the dielectric and elasticity models, respectively,

$$W_d(k) \equiv \omega(k) = \frac{-ig_d(x)k_x - i6r_d k^2 k_x}{ia_d(x)k^4 + ib_d(x)k^2 + c_d(x)k + m_d k^3}, \tag{30}$$

$$W_e(k) \equiv \omega(k) = \frac{ig_e k_x - 3d_e(x)kk_x}{a_e(x)k^3 - ib_e k^2 + h_e k}. \tag{31}$$

In Fig. 4 the real (oscillatory) frequency dependence versus applied field for the dielectric and elasticity models is illustrated. There are two facts that demand attention. First, for the dielectric model the frequency is negative, which means the waves travel from the right to the left towards the center of the localized region for $0<x<L$, and from the left to the right for $-L<x<0$. In other words, this model predicts the formation of a sink in the localized region. Second, the frequency for both models is in the order of tenths of Hz. In an experimental work [22], as discussed above, the authors reported counterpropagating waves along the director in dye-doped MBBA cells with tenths of Hz frequency. Therefore we assume that for arbitrarily small ramps $[df(x)/dx \ll 1$; see Fig. 1(b)] of the dielectric parameters we expect the formation of counterpropagating traveling waves inside a localized nonuniform region. Using the following equations

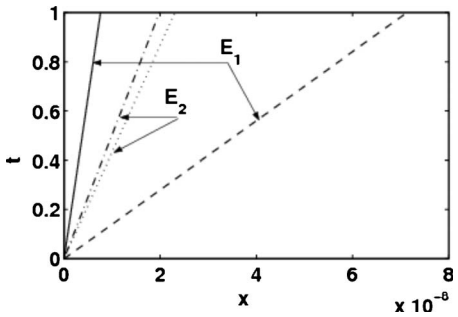

FIG. 5. Group and phase lines for elasticity model; solid line—group line, dashed line—phase line at $E_1=2$ statvolt/cm; dash-dot line—group line, dotted line—phase line at $E_2=10$ statvolt/cm.

$$\text{Abs}[\text{Re}(\omega(k))]/\text{Re}(k) = x/t_p,$$

$$\frac{d}{dk}\text{Abs}[\text{Re}(\omega(k))] = x/t_g, \tag{32}$$

we obtain the phase and group lines for the dielectric and elasticity models. Here t_p and t_g represent time for phase and group lines, respectively. In Figs. 5 and 6 the group and phase lines at two applied field values for dielectric and elasticity models are illustrated, respectively. For both models, as one can see, the phase velocity is larger than the group velocity. This indicates the fact that individual waves move faster than the wave's package. Also it is clear that with increase of the applied field the difference between both velocities decreases.

We assume that the temporal distortion angle oscillations for variable dielectric model are caused by the existence of a nonzero net x component of the reduced in dielectric medium electric field within one wavelength,

$$D_{x,net} = \int_0^{\lambda} \frac{\partial D_x}{\partial x} dx,$$

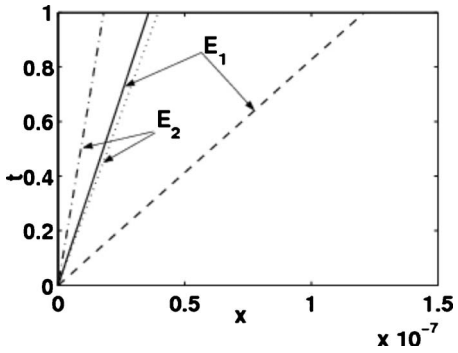

FIG. 6. Group and phase lines for dielectric model; solid line—group line, dashed line—phase line at $E_1=2$ statvolt/cm; dash-dot line—group line, dotted line—phase line at $E_2=10$ statvolt/cm.

$$\frac{\partial D_x}{\partial x} = D_{x0}[\varepsilon + ikf(x)]\exp(i\varphi),$$

$$D_{x0} = \varepsilon_p E_{x0} + E\varepsilon_a \theta_0,$$

$$D_x = D_{x0} f(x)\exp(i\varphi). \quad (33)$$

Here for simplicity once again (see above) we assume that the ramps of the dielectric parameters affect just the phase and not the amplitude of the distortion angle θ and x component of the applied field E_x. Hence in the equations,

$$\theta = \theta_0 \exp(i\varphi),$$

$$E_x = E_{x0} \exp(i\varphi), \quad (34)$$

the amplitudes θ_0 and E_{x0} are constants. Note that we obtain Eq. (33) by using Eq. (5) which relates D to E. In Fig. 7 a schematics of the periodic director pattern with charge separation for the dielectric model is illustrated. The net field causes space-charges displacement from the equilibrium positions. This motion is opposed by viscous and elastic terms. At some charges the resistance force overtakes the net electric field and pushes the charges back to the equilibrium positions. The process repeats, causing charges to drift forth and back periodically with time. The charges motion in turn generates periodic temporal oscillations of the distortion angle. For a uniform medium, as one can see from Eq. (33),

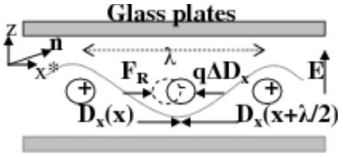

FIG. 7. Schematics of periodic director pattern with charge separation inside the ramp region for the variable dielectric model; $-q$ and $+q$ are induced by applied electric field E negative and positive space charges, respectively; $D_x(x)$ and $D_x(x+\lambda/2)$ are the x components of the reduced electric field vector at x and $x+\lambda/2$ coordinates, respectively; F_R is the resistance force with viscous and elastic terms; n is the nematic's director; sinusoidal line with λ wavelength represents the distribution of liquid crystal molecules.

the net x component of the reduced in size electric field over one wavelength is zero (the term in square brackets becomes one in this case). Hence the schematics depicted in Fig. 7 becomes a Carr-Helfrich-type instability (stationary Williams rolls) schematics, where $D_x(x)=D_x(x+\lambda/2)$ and space charges remain at the equilibrium positions [11,12,15]. Finally, it would be interesting to develop a two-dimensional model considering cell thickness also (z axis). This would be credible from the point of view of understanding and modeling the formation of patterns of a different nature in nonuniform liquid crystal media.

[1] M. A. Scherer and G. Ahlers, Phys. Rev. E **65**, 051101 (2002).
[2] D. Funfschilling, B. Sammuli, and M. Dennin, Phys. Rev. E **67**, 016207 (2003).
[3] T. John, U. Behn, and R. Stannarius, Phys. Rev. E **65**, 046229 (2002).
[4] W. I. Goldburg, Y. Y. Goldschmidt, and H. Kellay, Phys. Rev. Lett. **87**, 245502 (2001).
[5] M. Scheuring, L. Kramer, and J. Peinke, Phys. Rev. E **58**, 2018 (1998).
[6] N. Éber, S. Németh, A. G. Rossberg, L. Kramer, and Á. Buka, Phys. Rev. E **66**, 036213 (2002).
[7] S. Komineas, H. Zhao, and L. Kramer, Phys. Rev. E **67**, 031701 (2003).
[8] Á. Buka, B. Dressel, W. Otowski, K. Camara, T. Toth-Katona, L. Kramer, J. Lindau, G. Pelzl, and W. Pesch, Phys. Rev. E **66**, 051713 (2002).
[9] J.-H. Huh, Y. Hidaka, A. G. Rossberg, and S. Kai, Phys. Rev. E **61**, 2769 (2000).
[10] G. H. Heilmeier, L. H. Zanoni, and L. H. Barton, Proc. IEEE **56**, 1162 (1968).
[11] E. F. Carr, J. Chem. Phys. **39**, 1979 (1963).
[12] W. Helfrich, J. Chem. Phys. **51**, 4092 (1969).
[13] P. A. Penz and G. W. Ford, Phys. Rev. A **6**, 414 (1972).
[14] S. A. Pikin, Sov. Phys. JETP **33**, 641 (1971).
[15] W. J. A. Goossens, in *Advances in Liquid Crystals*, edited by G. H. Brown (Academic Press, New York, 1978), Vol. 3.
[16] M. Dennin, G. Ahlers, and D. S. Cannell, Science **272**, 388 (1996).
[17] M. Dennin, G. Ahlers, and D. S. Cannell, Phys. Rev. Lett. **77**, 2475 (1996).
[18] M. Dennin, D. S. Cannell, and G. Ahlers, Phys. Rev. E **57**, 638 (1998).
[19] M. Dennin, M. Treiber, L. Kramer, G. Ahlers, and D. S. Cannell, Phys. Rev. Lett. **76**, 319 (1996).
[20] A. Joets and R. Ribotta, Phys. Rev. Lett. **60**, 2164 (1988).
[21] H. R. Brand, C. Fradin, P. L. Finn, W. Pesch, and P. E. Cladis, Phys. Lett. A **235**, 508 (1997).
[22] N. C. Giebink, E. R. Johnson, S. R. Saucedo, E. W. Miles, K. K. Vardanyan, D. R. Spiegel, and C. C. Allen, Phys. Rev. E **69**, 066303 (2004).
[23] D. R. Spiegel, E. R. Johnson, and Skyler R. Saucedo, Phys. Rev. E **73**, 036317 (2006).
[24] E. L. Koschmieder, Adv. Chem. Phys. **32**, 109 (1975).
[25] J. P. Gollub, in *Nonlinear Dynamics and Turbulence*, edited by D. Joseph and G. Iooss (Pittman, New York, 1982).
[26] F. H. Busse, in *Hydrodynamic Instabilities and the Transition to Turbulence* (Springer-Verlag, Berlin, 1981).
[27] J. S. Langer, Rev. Mod. Phys. **52**, 1 (1980).
[28] M. Flicker and J. Ross, J. Chem. Phys. **60**, 3458 (1974).
[29] P. C. Fife, *Mathematical Aspects of Reacting and Diffusing Systems* (Springer-Verlag, Berlin, 1979).
[30] Y. Pomeau and P. Manneville, J. Phys. (Paris), Lett. **40**, 609 (1979).
[31] M. C. Cross, P. G. Daniels, P. C. Hohenberg, and E. D. Siggia, Phys. Rev. Lett. **45**, 898 (1980).
[32] Y. Pomeau and P. Manneville, Phys. Lett. **75A**, 296 (1980).

[33] Y. Pomeau and S. Zaleski, J. Phys. (Paris) **42**, 515 (1981).
[34] Y. Pomeau and P. Manneville, J. Phys. (Paris) **42**, 1067 (1981).
[35] M. C. Cross, P. G. Daniels, P. C. Hohenberg, and E. D. Siggia, Phys. Rev. Lett. **45**, 898 (1980).
[36] L. Kramer, E. Ben-Jacob, H. Brand, and M. C. Cross, Phys. Rev. Lett. **49**, 1891 (1982).
[37] P. M. Morse and H. Feshbach, *Methods of Theoretical Physics* (McGraw-Hill, New York, 1953).